HHS Public Access

Author manuscript

J Thromb Haemost. Author manuscript; available in PMC 2021 January 01.

Published in final edited form as:

J Thromb Haemost. 2020 January ; 18(1): 123–135. doi:10.1111/jth.14663.

Role of Thrombomodulin expression on hematopoietic stem cells

Sreemanti Basu[1], **H.P. Helena Liang**[1], **Irene Hernandez**[1], **Mark Zogg**[1], **British Fields**[1], **Jennifer May**[1], **Yamini Ogoti**[1], **Tine Wyseure**[2], **Laurent O. Mosnier**[2], **Robert T. Burns**[1], **Karen Carlson**[1,3], **Hartmut Weiler**[1,4]

[1]Blood Research Institute, BloodCenter of Wisconsin: part of Versiti, Milwaukee, WI, USA

[2]Department of Molecular Medicine, The Scripps Research Institute, La Jolla, CA.

[3]Division of Hematology and Oncology, Medical College of Wisconsin, Milwaukee, WI, USA

[4]Department of Physiology, Medical College of Wisconsin, Milwaukee, WI, USA

Abstract

BACKGROUND—Activation of protease-activated receptor 1 (PAR1) by either thrombin or activated protein C (aPC) differentially regulate the quiescence and bone marrow (BM) retention of hematopoietic stem cells (HSC). Murine HSC co-express Thbd, PAR1, and EPCR, suggesting that HSC sustain quiescence in a quasi-cell autonomous manner; due to the binding of thrombin present in the microenvironment to Thbd, activation of EPCR-bound protein C by the thrombin-Thbd-complex, and subsequent activation of PAR1 by the aPC-EPCR complex.

OBJECTIVE—To determine the role of Thbd expression on HSC for sustaining stem cell quiescence and BM retention under homeostatic conditions.

METHODS—HSC function was analyzed in mice with constitutive or temporally controlled complete Thbd-deficiency by flow cytometry, functional assays, and single cell RNA profiling.

RESULTS—Thbd was expressed in mouse, but not human HSC, progenitors, and immature B cells. Expression in vascular endothelium was conserved in humans BM. Mice with constitutive Thbd deficiency had a normal peripheral blood profile, altered BM morphology, reduced numbers of progenitors and immature B-cells, pronounced extramedullary hematopoiesis, increased HSC frequency and marginally altered transcriptionally defined HSC stemness. Transplantation experiments indicated near normal engraftment and repopulating ability of Thbd-deficient HSC. Transgenic aPC supplementation normalized BM histopathology and HSC abundance, and partially restored transcriptional stemness, but had no effect on B cell progenitors and extramedullary hematopoiesis. Temporally controlled Thbd gene ablation in adult mice did not cause the above abnormalities.

Corresponding Author: Hartmut Weiler, Blood Research Institute, Versiti (formerly BloodCenter of Wisconsin), 8727 Watertown Plank Road, Milwaukee WI 53226, Pho: 414-937-3813, Facs: 414-937-6284, hweiler@versiti.org.

Authorship: All authors designed and performed experiments and analyzed data. R.T.B. analyzed and interpreted single-cell RNA sequencing data. H.W. designed and coordinated the study.

The authors declare no conflicts of interest.

CONCLUSION—Thbd expression on HSPC has minor effects on homeostatic hematopoiesis in mice, and is not conserved in humans.

Keywords

Thrombomodulin; Hematopoiesis; Stem cells; Thrombosis; Hemostasis

Introduction

Several lines of evidence indicate that the activation state of the blood coagulation system affects the function of hematopoietic stem and progenitor cells (HSPC; reviewed in[1]). Thrombin-cleaved osteopontin regulates the proliferation, differentiation, and bone marrow (BM) retention of HSPC by activating β1 integrins[2, 3]; and thrombin-mediated activation of complement factor C5 augments the G-CSF-induced mobilization of HSPC[4, 5]. Factor VIII-deficient mice with reduced capacity for generating thrombin show enhanced HSC mobilization by G-CSF, but diminished abundance of HSC with long-term repopulating activity (LT-HSC), likely caused by diminished signaling via the thrombin receptor, protease activated receptor 1 (PAR1), on BM stromal cells[6]. Both FVIII- and PAR1-knockout mice showed decreased bone mass, aberrant BM architecture, and diminished BM plasma levels of CXCL12 protein[6], which is required for BM retention of HSC[7]. Experimental infusion of excess thrombin triggered HSC egress from the BM, via PAR1 activation on stromal cells and/or HSC[8]. HSC retention in the BM was spontaneously enhanced in mice with low expression of the endothelial protein C receptor, EPCR (gene symbol: Procr), and in mice lacking PAR1 ($PAR1^{NULL}$). This suggested, first, that BM retention and quiescence of HSC are regulated by differential PAR1activation by either thrombin or activated protein C (aPC), where PAR1 activation by the aPC-EPCR complex promotes retention and quiescence, whereas thrombin-PAR1 signaling promotes HSC depletion from the BM, increased nitrous oxide (NO) production, and shedding of EPCR[8]. Second, these data indicated that low levels of thrombin generated constitutively in the HSC microenvironment provide physiologically relevant modulation of HSPC function via aPC-biased PAR1 signaling in the absence of additional hematopoietic stress signals. The balance of thrombin- versus aPC-biased PAR1 signaling is largely determined by the bioavailability and activity of the essential co-factor for the thrombin-mediated activation of protein C, Thbd. Mouse HSC co-express EPCR, PAR1, and Thbd[8], and therefore have the capacity to sustain Thbd/thrombin-mediated aPC generation and constitutive aPC-EPCR-PAR1 signaling in a quasi-autocrine manner. Consistent with this notion, mice with reduced capacity for protein C activation due to a point mutation in Thbd ($Thbd^{PRO}$-mice) were reported to exhibit a spontaneous loss of HSC from the BM under homeostatic conditions. i.e. in the absence of acute experimental challenges such as infusion of thrombin;[8]. Here, we further investigate the function of Thbd expression on HSC in steady-state hematopoiesis in mice.

Materials And Methods

Mice:

C57BL/6N, C57BL/6J, and B6.SJL-*Ptprc*^{a}*pepc*^{b}/BoyJ mice were from Charles River Laboratories (Wilmington, MA) and Jackson Laboratories (Bar Harbor, ME). Cpb2-deficient

mice, Meox2Cre-Thbd^{DEL}, ERCre-Thbd^{DEL} and APC^{HI}-mice were described[9, 10]. Except for Cpb2-defcient mice (C57BL/6J), mice were on a C57Bl/6N background. Animals were housed in the specific pathogen-free facility of Translational Biomedical Research Center of the Medical College of Wisconsin, and HSPC analyses were performed approximately 2h after the initiation of the light cycle[11]. Procedures were approved by the Medical College of Wisconsin Institutional Animal Care and Use Committee.

Human samples:

Whole BM and GCSF-mobilized peripheral blood mononuclear cells from healthy human subjects were purchased from All Cells (Alameda, CA). BM sections were collected with approval by the Medical College of Wisconsin's Institutional Review Board (PRO00025731) from archived formalin fixed trephine BM biopsies from adult patients with hematologic malignancies (Thbd-stained sample: diffuse large B cell lymphoma; marrow without evidence of malignancy on clinical hematopathologist review. EPCR-stained sample: primary myelofibrosis).

Reagents:

Anti- mouse Ter119-BV421, Sca-1-APC, CD34-FITC, CD135-PE, IL-7Ra-BV605, CD48-FITC, CD150-PE Cy7, CD45.2-Alexa Fluor 700/APC Cy7, CD11b-BV605, CD3-APC, NK1.1-APC Cy7, CD19-BV605, IgM-Alexa Fluor 647, CD43-PE Cy7, CD16/32-PerCP Cy5.5, CD16/32; anti-human CD34-APC Cy7 (clone: 581), CD38-PE Cy7 (HB-7), CD45RA-BV 605 (HI100), CD90-APC (5E10), CD49f-PerCP Cy5.5 (GoH3), CD45-PE/Dazzle 594 (HI30), and CD33-APC (P67.6) antibodies; and Legendplex™ Mouse Inflammation Panel (13-plex) and Mouse IL-6 ELISA were purchased from Biolegend (San Diego, CA). IL6 depleting AB (clone MP5–20F3) from BioXCell (West Lebanon, NH).

Anti-mouse c-Kit-PE Cy7, Mouse Hematopoietic Lineage Biotin Panel, and anti-human CD19-Alexa Fluor 700 (HIB19) from eBioscience (San Diego, CA). Anti-B220-PE CF594 from BD biosciences (San Jose, CA). EasySep Human Progenitor Cell Enrichment Kit from Stem Cell Technologies Inc. (Vancouver, BC). Anti-human EPCR-FITC (RCR-49) from Santa Cruz Biotechnology®, inc. (Dallas, TX). Anti-human CD141-PE (AD5–14H12) from Miltenyi Biotec Inc. (Auburn, CA).

Flow cytometry:

Single cell suspension from BM (femur and tibia) were prepared by flushing cells, and passing through an 18 G needle. Spleen single cell suspensions were prepared by mincing on 70 μm nylon mesh cell strainer. Cells were labeled with antibodies followed by incubation with anti-CD16/32 (Fc-block) or anti-CD16/32-PerCP Cy5.5 (for mouse precursor analysis). Lineage- (Ter119, B220, CD3, Gr1) negative mouse HSPC populations were characterized as MPP: LSK-CD34^{POS}CD135^{POS}; CLP: Lin^{NEG}Sca-1^{LO}c-Kit^{LO}IL7Ra^{POS}; CMP: Lin^{NEG}Sca-1^{NEG}c-Kit^{POS}CD34^{POS}CD16/32^{NEG}; GMP: Lin^{NEG}Sca-1^{NEG}c-Kit^{POS}CD34^{POS}CD16/32^{POS}; MEP: Lin^{NEG}Sca-1^{NEG}c-Kit^{POS}CD34^{NEG}CD16/32^{NEG}. Pro-B: CD19^{POS}B220^{LO}IgM^{NEG}CD43^{POS}; pre-B: CD19^{POS}B220^{LO}IgM^{NEG}CD43^{NEG}; immature B: CD19^{POS}B220^{LO}IgM^{POS}; mature B: CD19^{POS}B220^{HI}IgM^{POS}. Human BM and GCSF-mobilized peripheral blood mononuclear cells were enriched for progenitors by

using EasySep Human Progenitor Cell Enrichment Kit (StemCell Technologies, Vancouver, BC), and characterized by expression of CD34, CD38, CD45RA, CD90, CD49f as described[12].

Colony forming assay:

Immediately after euthanasia, single cell suspension from BM or spleen in Iscove's MDM / 2% FBS (Stem Cell Technologies; Vancouver, BC) were prepared and enumerated using a SCil Veterinarian ABC Hematology Analyzer (Gurnee, IL). Cells were plated at a density of 4×10^4 (BM) or 4×10^5 cells (spleen) per 35 mm tissue culture dish in granulocytic precursor-specific methylcellulose (Catalog #: M3534; Stem Cell Technologies; Vancouver, BC). CFU-GM were determined 7–10-days after plating.

Immunohistochemistry:

Rehydrated Paraffin-embedded sections were treated for 30 minutes (steam) in Epitope Unmasking Solution (BioWorld; Dublin, OH), blocked with a 4:4:1:2 mixture of Tris-buffered saline, NoProteinBlock (VWR, Radnor, PA), Innovex FC Receptor Block (Fisher, Pittsburgh, PA), and 2.5% Horse serum (Vector labs, Burlingame, CA), and incubated at 4°C overnight with primary antibodies (sheep anti-human Thbd: AF3947; goat anti-mouse Thbd: AF3894; goat anti-human EPCR: AF2245; R&D Systems, Minneapolis, MN; goat-anti mouse EPCR; kind gift from Dr. Charles Esmon, Oklahoma Medical Research Foundation, Oklahoma City, OK) diluted in blocking solution. Samples were incubated at 37°C for thirty minutes with secondary antibodies (donkey anti-goat IgG Alexa Fluor 488 (#A-11055) and donkey anti-sheep IgG Alexa Flour 594 (#A-11016), Invitrogen/Life Technologies; Waltham, MA; ImmPRESS horseradish peroxidase (HRP)-conjugated horse anti-Goat IgG Polymer Detection Kit, #MP-7405; or donkey anti-goat HRP conjugate and detection with ImmPACT NovaRED Peroxidase (HRP) substrate; Vector Laboratories, Burlingame, CA). Images were captured on a Nikon Eclipse E600 microscope equipped with a Diagnostic Instruments Color Mosaic 11.2 digital camera and Plan Fluor 20x (057802) objective. Immunofluorescence was imaged using a Nikon Ti-2 E inverted microscope with CFI Plan APO Lambda 20x and CFI Plan APO Lambda 40x objectives. Images were optimized for reproduction by adjusting brightness using Powerpoint Utilities (Microsoft) without further modifications.

BM transplantation:

Mixed BM chimera mice were generated by intravenous infusion of 1×10^6 CD45.1 BM cells together with either 1×10^6 Thbd-null, or 1×10^6 $Thbd^{lox/+}$ BM cells (CD45.2) into lethally irradiated (9 Gy; single dose, GammaCell 40, MDS Nordion) congenic CD45.1 C57/BoyJ recipient mice 20h after irradiation. Drinking water for recipients was supplemented with 1.25 mg/mL of sulfadiazine/trimethoprim for 4 weeks and the flow cytometric analyses were performed after 12–16 weeks.

Single Cell RNA Sequencing and Bioinformatics Analysis:

Single-cell RNA-sequencing libraries were prepared from sorted LSK cells using the Chromium Controller and Single Cell 3′ v2 Reagent Kit (10x Genomics) according to

manufacturer's protocol, and sequenced on an Illumina NextSeq 500 with the NextSeq 500/550 High Output Kit v2 (Ilumina, San Diego, CA; 150 cycles; read1 26 cycles, read 2 98 cycles, i7 index 8 cycles). Demultiplexing, alignement to the *Mus musculus* mm10 genome, and UMI sums for each gene were quantified using 10X Genomics Cell Ranger v2.2.0. Filtered barcode matrix files were imported into the Seurat v2.3.4 single cell analysis package[13] using R v3.5.2 (R Core Team, 2018; http://www.R-project.org/). Cells expressing fewer than 200 genes, cells with >7.5% contribution of mitochondrial genes, and genes expressed in fewer than 3 cells were filtered out. Gene expression values for each cell were log-normalized and scaled by a factor of 10,000 based on the number of UMIs in each cell and the cell mitochondrial content. Cell cycle phase was predicted as described[14]. Genes with high dispersion in at least two samples were used to conduct canonical correlation analysis to group the sub-populations of cells from each sample together[15]. The first twenty canonical correlation vectors were chosen for downstream clustering and visualization based on their shared correlation strengths and the genes driving each canonical correlation vector. Naïve clustering of the cells into sub-populations was then conducted using Seurat's implementation of a shared nearest neighbor (SNN) modularity optimization based clustering algorithm (Louvain's original algorithm[16]). The sample populations were aligned using these canonical correlation vectors and visualized using a uniform manifold approximation and projection plot (UMAP)[17]. Differentially expressed genes between clusters or samples were determined using Wilcoxon rank sum tests and Bonferroni correction. HSC, MolO, and SuMO module scores were calculated for every cell as described[14]. Raw FastQ files and gene expression data will be accessible at NCBI SRA and GEO; accession # pending).

Statistical analyses:

Unless specified differently in the results section, two-tailed unpaired t-test or two-tailed Mann-Whitney test was performed to compare the WT and $Thbd^{DEL}$ groups. One-way ANOVA with Tukey's *post hoc* test was used to compare multiple groups.

Results

Expression of Thbd and EPCR on mouse hematopoietic progenitor cells

To identify HSPC capable of Thbd-dependent EPCR-aPC-PAR1 signaling, we examined the expression patterns of Thbd and EPCR in 12–20 week old wildtype (C57Bl6/N) mice. Confirming earlier reports[8], Thbd was expressed by $Lineage^{NEG}Sca\text{-}1/c\text{-}Kit^{POS}$ (LSK)-$CD150^{POS}CD48^{NEG}$ HSPC; Thbd abundance was similar in LSK-$CD34/CD135^{NEG}$, or $EPCR^{POS}$ Hoechst side population cells Figure 1A). Thbd was also expressed in ST-HSC (LSK-$CD34^{POS}CD135^{NEG}$), multipotential, and lineage-biased progenitors (MPP, CLP, CMP, GMP), and in a subpopulation of MEP (Figure 1B). Approximately half of BM-resident $B220/CD19^{POS}$ B cells/B cell precursors showed Thbd expression, as reported earlier[18]. The fraction of B cells expressing Thbd correlated inversely with B cell maturation: Between 70 and 90% of Pro- and Pre-B cells, but only half of immature B cells expressed Thbd, and expression by mature B cells was nearly undetectable (Figure 1C). EPCR was detected on the majority of LT-HSC (LSK-$CD150^{POS}CD135/CD34/CD48^{NEG}$), approximately $1/3^{rd}$ of $CD34/CD150^{POS}CD135/CD48^{NEG}$ ST-HSC / MPP1 cells and

CD150^{NEG}CD135/CD34/CD48^{POS} MPP4 cells, and small subpopulations of CD34/CD48/CD150^{POS}CD135^{NEG} MPP2 and CD34/CD48^{POS}CD135/CD150^{NEG} MPP3 cells. EPCR expression was highest in LT-HSC and approximately ½ of this level in progenitors. The myeloid-primed CD41^{POS} HSC subset[19] also showed EPCR surface expression in both older and younger mice (9 or 2 months; Figure 1D). EPCR was undetectable on B cells (data not shown).

Constitutive Thbd-deficiency is associated with altered composition of the hematopoietic progenitor pool

Selective preservation of Thbd expression in the placenta enables the derivation of live animals with near-complete Thbd-deficiency (MeoxCre-Thbd^{DEL} mice), yet these mice exhibit partial perinatal lethality, reduced body size/weight, a marked prothrombotic diathesis, limited life span, yet a normal peripheral blood hematologic profile[9]. 4 of 5 l Thbd^{DEL} mice exhibited fibrosis in the epiphyseal BM and increased fat cell abundance (Figure 2A). All Thbd^{DEL} mice displayed ~1.5 fold reduced BM cellularity relative to body mass (Figure 2B). The relative abundance of BM-resident CD34/CD135^{NEG} LT- and CD34^{POS}CD135^{NEG} ST-HSC was increased, while CLP were diminished (Figure 2C). Absolute numbers of LT- and ST-HSC normalized to body weight were comparable to wildtype controls, whereas CLP and to a lesser extent GMP were diminished (Figure 2C). The abundance of MPP, CMP and MEP remained identical to that of wildtype animals. Absolute numbers of Pro-, Pre-, immature, and mature B cells were reduced more than 2-fold, without altering the relative abundance of each population (Figure 2D). EPCR expression on LT-HSC of Thbd^{DEL} mice was indistinguishable from Thbd-expressing littermates (Figure 2E). The spleen of Thbd^{DEL} mice showed increased weight and cellularity, increased frequency and numbers LSK-cells, LT-HSC, and GMP, and yielded larger numbers of CFU-GM in methylcellulose cultures (Figure 2F). No increase in circulating progenitors was detectable in peripheral blood, as judged from methylcellulose assays. Analysis of SLAM-HSC in wildtype (average age: 3.5 months) and Thbd^{DEL} mice (average age: 6.6 months) likewise showed increased abundance of HSC in the latter that correlated with increased representation of CD34/CD135^{NEG} LT-HSC amongst the SLAM-HSC pool (Figure 2G). Equivalent results were obtained for HSC gated as CD48^{NEG}CD150/EPCR^{POS} E-SLAM HSC (wildtype: 5.2±0.6; Thbd^{DEL}: 17.7±5.9; mean±SEM; n=5/group). Thbd^{DEL} CD34/CD135^{NEG} LT-HSC had normal proliferation, yet reduced apoptosis, as judged from Ki67 and annexin V staining, respectively (Figure 2H).

Thbd-deficient stem and progenitor cells exhibit near-normal hematopoietic repopulation activity

The functional role of HSPC-associated Thbd was assessed by transplanting equal numbers of wildtype CD45.1^{POS} competitor cells and CD45.2^{POS} BM cells from Thbd^{DEL}, or Thbd-expressing Thbd$^{LOX/WT}$ controls into lethally irradiated Boy/J recipients. To correct for differences in the relative frequencies of LT-HSC in Thbd$^{LOX/WT}$ and Thbd^{DEL} mice, donors with a ≤1.2-fold difference in absolute numbers of LSK-CD34^{NEG}CD135^{NEG} HSC were selected. 16–20 weeks after transplantation, Thbd-expressing and Thbd-deficient CD45.2 cells contributed similarly to all BM mononuclear cells and the B cell/B cell precursor pool, with marginal under-representation amongst LT-HSC, CLP, and B-cells (Figure 3A).

Thbd^{DEL} and control cells likewise were represented identically in peripheral blood T, B, and myeloid cells and among spleen LSK, GMP, and CD11b^{+} myeloid compartments (Figure 3B,C).

Temporally controlled Thbd gene ablation in adult mice preserves normal HSPC abundance and bone marrow retention

Thbd gene ablation in 2 months old adult healthy animals was induced by tamoxifen-treatment of conditional Thbd-knockout mice (ERCre-Thbd^{FLOX}). The loss of Thbd expression in BM endothelial and LSK cells was ascertained by immunohistochemistry and flow cytometry, respectively, in 5 animals that had remained free of thrombotic complications over 6 months following tamoxifen treatment as described[9] (Figure 4A,B). Body and spleen weights, BM cellularity and histological appearance, and the relative abundance of HSC defined as the Hoechst-excluding LSK-side population (Figure 4C) or as LSK-CD34/CD135^{NEG} (not shown), were identical to controls not treated with tamoxifen. Hematopoietic activity in the BM, as judged from CFU-M assays, was somewhat reduced ($p=0.037$), and non-significantly elevated in the spleen and peripheral blood (Figure 4D).

Transgenic supplementation of APC selectively restores normal HSPC abundance

To determine whether the hematopoietic abnormalities in Thbd^{DEL} mice could be rescued by augmented protein C activation, Meox2Cre-Thbd^{DEL} mice were bred with a transgenic mouse strain (mAPC^{HI}) expressing the D168F/N173K mouse analogue of the hyper-activatable human D167F/D172K protein C variant[9, 20]. Transgene–mediated aPC delivery results in 2- and 3-fold increased plasma levels of murine PC and aPC, respectively, ameliorates the growth retardation and prothrombotic phenotype of Thbd^{DEL} mice, and enables symptom-free long-term survival of the majority of Thbd^{DEL} mice[9]. Transgenic aPC supplementation partially normalized the abundance of CD34/CD135^{NEG} LT-HSC, SLAM- and E-SLAM HSC in Thbd^{DEL} mice, but did not correct the diminished abundance of CLP and B cell precursors, or the pronounced spleen hematopoietic activity, and had no effect on HSC in otherwise normal mice (Figure 5A–C). Of note, plasma IL6 levels remain elevated in Thbd^{DEL}APC^{HI} mice[9]. Given the reported effects of IL6 signaling on extramedullary hematopoiesis, B cell maturation, and SDF secretion[21–23], the role of IL6 was evaluated by treating animals for 3 weeks with IL-6-blocking antibodies. Plasma IL-6 remained undetectable 4 days after the last antibody infusion, but IL-6 neutralization did not correct the B cell defects, or diminish spleen hematopoietic activity. To examine whether the above defects may be attributed to diminished activation of plasma carboxypeptidase B2 (gene symbol: Cpb2) by the thrombin-Thbd complex and the ensuing altered complement function, Cpb2-deficient mice were analyzed. Cpb2-deficient mice, compared to wildtype C57BL/6N or J mice, showed normal cellularity of the spleen and bone marrow, normal abundance of bone marrow-resident HSPC and B-cell progenitors, and normal hematopoietic activity in the spleen (data not shown).

Thbd^{DEL} HSC exhibit near-normal transcriptionally defined stemness

Duplicate samples of LSK cells were collected from C57Bl6/N wildtype, Thbd^{DEL}, and Thbd^{DEL}APC^{HI} mice and subjected to single-cell RNA sequencing. Naive clustering analysis of the pool of 6 samples resolved 10 distinct populations (Figure 6A). LT-HSC

("HSC"; cluster 2) were identified by low/absent expression of CD48, FLT3, and CD34, enrichment for EPCR and CD150 (Figure 6B), above-average MolO and SuMO stemness scores based on a common RNA expression profile of 29 and 21 genes, respectively, in index-sorted *bona fide* HSC[24] (Figure 6C), and a high proportion of quiescent cells (G0/G1) as estimated from expression of 97 cell cycle-dependent RNAs[14] (Figure 6D). The proliferative status of cells allocated to all individual clusters, including the HSC cluster 2, was comparable for all mouse strains (Figure 6D). The abundance of LT-HSC in $Thbd^{DEL}$ mice as defined by contribution to cluster 2, as well as overall (all LSK cells) allocation to non-HSC clusters were comparable between strains, indicating similar transcriptional stratification of the LSK pool (Figure 6E). Mean MolO stemness scores for the cluster 2 HSC populations were similar across strains (wildtype: 0.011; $Thbd^{DEL}$: −0.008; $Thbd^{DEL}$-APC^{HI}: −0.024; *p=0.12*) (Figure 6F). A more comprehensive HSC scoring module was extracted from a set of 424 genes whose expression was on average 1.2-fold higher ("HSC_up score") or lower ("HSC_down score") in cluster 2 than in all other clusters in wildtype mice (adjusted p<0.01; supplemental file 1). $Thbd^{DEL}$ HSC showed mildly lower HSC_up and higher HSC_down scores, respectively, while $Thbd^{DEL}$-APC^{HI} showed an intermediate value (HSC_up: wildtype 0.41; $Thbd^{DEL}$: 0.35; $Thbd^{DEL}$-APC^{HI}: 0.38. HSC_down: wildtype: 0.25; $Thbd^{DEL}$: 0.33; $Thbd^{DEL}$-APC^{HI}: 0.32; *p<0.0001* for both up and down scores) (Figure 6F). Approximately 5% of $Thbd^{DEL}$ HSC (25 of 540; circled in Figure 6F) showed markedly aberrant HSC_up/down scores, increased numbers of transcripts and number of genes detected, and entry into S (n=4) or G2M (n=21) cell cycle phases, indicating transcriptional activation and loss of quiescence.

Human hematopoietic stem and progenitor cells do not express Thbd

Immunohistochemical analysis of human BM biopsies from healthy donors showed Thbd and EPCR expression in vascular endothelial cells, indicating that Thbd expression in the vascular HSPC niche is conserved between species (Figure 7A). HSPC populations in human bone marrow were characterized by flow cytometry according to established gating protocols[12] (Figure 7B). Except for a small fraction of $CD33^{POS}$ myeloid cells, Thbd was undetectable in BM mononuclear cells, including HSPC enriched in LT-HSC (Lin/CD38/$CD45RA^{NEG}$$CD90$/CD34/$CD49f^{POS}$ and Lin/CD38/CD45RA/$CD90^{NEG}$CD34/$CD49f^{POS}$), MPP, other CD34/$CD38^{POS}$ progenitors, or $CD19^{POS}$ B cells. (Figure 7C). EPCR-expression in human BM HSPC was limited to a subpopulation of presumptive $CD90^{POS}$ HSC (Figure 7C, right panels). A corresponding analysis of peripheral blood from healthy GCSF-mobilized donors failed to detect EPCR or Thbd expression in putative HSC and progenitors, with the exception of Thbd-expression in myeloid populations (Figure 7D).

Discussion

The current work examined the potential function of Thbd in the regulation of aPC- or thrombin-biased PAR1 signaling on HSPC. We confirmed Thbd expression on *bona fide* LT-HSC and BM-resident B cells[8, 18], but in addition found Thbd expressed on all murine HSPC and lineage-committed precursors, as well as B cell precursors. Thus, in the mouse, approximately 25% of all BM-resident mononuclear cells express Thbd on their surface, providing a substantial capacity for protein C activation. EPCR expression was detected in

LT-HSC and ~1/3rd of ST-HSC and MPP, but not in B cell progenitors. In humans, Thbd expression in the BM was limited to vascular endothelium, while EPCR was expressed in a subset of presumptive HSC, and in vascular endothelium. In both mice and humans, the highest levels of PAR1 mRNA have been measured in HSC-enriched fractions, yet are almost 1 order of magnitude lower in B cells [25, 26]. Taken together, the analysis of EPCR and Thbd expression document the potential for quasi-autocrine EPCR-aPC-PAR1 signaling in mouse LT-HSC, ST-HSC, and to a lesser extent MPP, whereas in human BM such a mechanism is likely limited to the endothelial component of the BM niche.

Hematopoietic abnormalities in $Thbd^{DEL}$ mice included altered BM morphology and cellularity, increased relative abundance, but normal absolute numbers of HSC relative to body mass, marked extramedullary hematopoietic activity in the spleen, subtle skewing of committed progenitors towards myeloid lineages and significantly reduced abundance of B cell progenitors. The B cell defect was already manifest at the Pro-B cell stage and therefore likely reflected diminished B cell lineage output by CLP. The mechanisms underlying CLP and B cell precursor abnormalities remain unknown, but the absence of EPCR and limited expression of PAR1 in the human and mouse B cell lineage render a role of B cell-expressed Thbd in B cell differentiation via biased EPCR/PAR1 signaling unlikely. Transgenic supplementation of aPC prevented thrombo-hemorrhagic perinatal lethality, provided systemic anticoagulation, enabled thrombosis-free survival of $Thbd^{DEL}$ mice[9], normalized BM histology and relative abundance of HSC, but did not prevent extramedullary hematopoiesis or abnormal B cell precursor abundance. These outcomes provided indirect evidence that the hematopoietic effects of Thbd-deficiency on BM retention of HSC and B cell precursor abundance are not caused by the loss of aPC-mediated anticoagulant function. However, due to competition of circulating aPC and protein C for binding to EPCR (see below), the failure of transgenic aPC to correct these abnormalities may not be fully informative about the role of aPC-mediated cell signaling. Activation of plasma carboxypeptidase B by the thrombin-Thbd complex likewise was not necessary for sustaining HSC BM retention and normal B cell precursor abundance under homeostatic conditions. Alternatively, these effects of Thbd gene ablation might reflect aPC- and carboxypeptidase-independent Thbd functions, such as HMGB1 signaling or control of complement activation, which is known to affect hematopoietic function (reviewed in [27]).

Several additional experimental approaches yielded only limited evidence supporting the notion that HSC-expressed Thbd affects baseline hematopoietic function in a physiologically relevant manner. First, neither constitutive, nor temporally controlled Thbd gene ablation was associated with diminished or skewed hematopoietic lineage contribution to peripheral blood mononuclear cell, platelet, or erythrocyte abundance. The observed defects in BM-resident HSPC therefore do not disrupt the overall hematopoietic output. Second, no HSC derangements or extramedullary hematopoiesis were observed, when Thbd gene ablation was induced in adult healthy ERCre-$Thbd^{LOX}$ mice, despite the eventually similar prothrombotic diathesis and mortality upon tamoxifen treatment as seen in mice with constitutive Thbd deficiency[9]. Although differences in the efficacy of Cre-mediated gene deletion may contribute to the less pronounced effects of temporally induced Thbd ablation, the hematopoietic effects of constitutive Thbd deficiency nevertheless are likely predominantly caused by a progressive pathology originating at birth, rather than the acute

loss of Thbd regulatory function in biased PAR1 signaling. Third, competitive BM transplants revealed only marginally compromised multi-lineage repopulation and/or engraftment by Thbd^{DEL} HSPC. While this finding does not support a dominant role of HSC-expressed Thbd, the reduced stem cell activity of CD45.1 cells in these competitive repopulation experiments might have masked more subtle defects of Thbd-deficiency. Fourth, while increased spleen hematopoietic activity provided indirect evidence for compromised BM retention of HSPC in mice with constitutive Thbd-deficiency, steady-state HSC abundance in BM was not diminished. This observation contrasted the reported loss of SLAM HSC in Thbd^{PRO} mice with diminished Thbd function[8], potentially reflecting confounding environmental influences, subtle genetic differences in strain backgrounds, other factors such as the microbiome, or replenishment of the BM-resident HSC pool by recirculating Thbd^{DEL} HSC. Fifth, single-cell RNA sequencing as an independent approach to characterize functional differences between HSC populations revealed only subtle, albeit significant, changes in transcriptionally defined stemness of Thbd^{DEL} HSC that were partially rescued by transgenic aPC supplementation. In summary, we conclude that a severe prothrombotic state due to constitutive or temporally controlled Thbd gene ablation is not sufficient to replicate the depletion of BM-resident HSC triggered by acute experimental thrombin infusion, or by the constitutive loss of PAR1 or EPCR function[8]; and (2) that expression of Thbd on murine HSC and progenitors has little, if any effect on the ability of HSC to maintain a normal hematopoietic output under normal physiologic conditions. These findings are largely consistent with independent analyses indicating a limited role of aPC-EPCR signaling on HSPC for hematopoiesis, such as in mice harboring a variant of EPCR with impaired ability to bind protein C[28], as well as the failure of signaling-selective aPC variants to reproduce the radio-protective effects of normal aPC[18]. Whether aPC generated by the Thbd/thrombin complex on the vascular endothelium can efficiently engage EPCR-PAR1 signaling on nearby HSC in a “paracrine” manner remains somewhat unclear: Ambient aPC levels are ~1000-fold lower than circulating zymogen protein C, and EPCR exhibits comparable affinity for protein C and aPC[29]. The majority of EPCR is therefore occupied by protein C under homeostatic conditions, and engagement of EPCR by circulating aPC is disadvantaged, even at the supra-physiologic levels achieved in APC^{HI} mice. However, on cells co-expressing Thbd, EPCR, and PAR1, EPCR-bound protein C provides a spring-loaded signaling complex that is readily engaged by sequestration of thrombin by Thbd, activation of EPCR-bound protein C by the thrombin-Thbd complex, and the “pseudo-autocrine” activation of PAR1 by EPCR-bound aPC. This mechanistic difference in triggering aPC-EPCR signaling might also explain why increasing the circulating level of aPC in APC^{HI} mice does not ameliorate extramedullary hematopoiesis in the spleen.

In summary, in the BM of mice, as well as humans, who lack Thbd expression on HSPC, a potential cell-autonomous, or quasi-autocrine function of HSC-expressed Thbd in the regulation of hematopoiesis via aPC-EPCR biased PAR1 signaling appears unlikely.

Supplementary Material

Refer to Web version on PubMed Central for supplementary material.

Acknowledgements:

The authors would like to thank the staff of the Blood Research Institute's Core Facilities for their support and technical expertise in flow cytometry, FACS sorting, sequencing, and Image acquisition. This work was supported by grants from the National Institutes of Health, National Heart, Lung and Blood Institute (HL117132; HL133348, HW), National Institute of Allergy and Infectious Diseases (AI133561, HW), the Ziegler Family Chair for Research (HW), (HL130678, HW and LOM), (HL142975; HL104165, L.O.M), American Heart Association Western States Postdoctoral Fellowship (TW), and K08HL127187 (K.C).

LITERATURE CITED

1. Nguyen TS, Lapidot T, Ruf W. Extravascular coagulation in hematopoietic stem and progenitor cell regulation. Blood. 2018; 132: 123–131. [PubMed: 29866813]
2. Grassinger J, Haylock DN, Storan MJ, Haines GO, Williams B, Whitty GA, Vinson AR, Be CL, Li S, Sorensen ES, Tam PP, Denhardt DT, Sheppard D, Choong PF, Nilsson SK. Thrombin-cleaved osteopontin regulates hemopoietic stem and progenitor cell functions through interactions with alpha9beta1 and alpha4beta1 integrins. Blood. 2009; 114: 49–59. [PubMed: 19417209]
3. Nilsson SK, Johnston HM, Whitty GA, Williams B, Webb RJ, Denhardt DT, Bertoncello I, Bendall LJ, Simmons PJ, Haylock DN. Osteopontin, a key component of the hematopoietic stem cell niche and regulator of primitive hematopoietic progenitor cells. Blood. 2005; 106: 1232–1239 [PubMed: 15845900]
4. Borkowska S, Suszynska M, Wysoczynski M, Ratajczak MZ. Mobilization studies in C3-deficient mice unravel the involvement of a novel crosstalk between the coagulation and complement cascades in mobilization of hematopoietic stem/progenitor cells. Leukemia. 2013; 27: 1928–1930. [PubMed: 23511127]
5. Borkowska S, Suszynska M, Mierzejewska K, Ismail A, Budkowska M, Salata D, Dolegowska B, Kucia M, Ratajczak J, Ratajczak MZ. Novel evidence that crosstalk between the complement, coagulation and fibrinolysis proteolytic cascades is involved in mobilization of hematopoietic stem/progenitor cells (HSPCs). Leukemia. 2014; 28: 2148–2154. [PubMed: 24667943]
6. Aronovich A, Nur Y, Shezen E, Rosen C, Zlotnikov Klionsky Y, Milman I, Yarimi L, Hagin D, Rechavi G, Martinowitz U, Nagasawa T, Frenette PS, Tchorsh-Yutsis D, Reisner Y. A novel role for factor VIII and thrombin/PAR1 in regulating hematopoiesis and its interplay with the bone structure. Blood. 2013; 122: 2562–2571. [PubMed: 23982175]
7. Sugiyama T, Kohara H, Noda M, Nagasawa T. Maintenance of the hematopoietic stem cell pool by CXCL12-CXCR4 chemokine signaling in bone marrow stromal cell niches. Immunity. 2006; 25: 977–988. [PubMed: 17174120]
8. Gur-Cohen S, Itkin T, Chakrabarty S, Graf C, Kollet O, Ludin A, Golan K, Kalinkovich A, Ledergor G, Wong E, Niemeyer E, Porat Z, Erez A, Sagi I, Esmon CT, Ruf W, Lapidot T. PAR1 signaling regulates the retention and recruitment of EPCR-expressing bone marrow hematopoietic stem cells. Nat Med. 2015; 21: 1307–1317. [PubMed: 26457757]
9. van Mens TE, Liang HH, Basu S, Hernandez I, Zogg M, May J, Zhan M, Yang Q, Foeckler J, Kalloway S, Sood R, Karlson CS, Weiler H. Variable phenotypic penetrance of thrombosis in adult mice after tissue-selective and temporally controlled Thbd gene inactivation. Blood Adv. 2017; 1: 1148–1158. [PubMed: 28920104]
10. Wyseure T, Cooke EJ, Declerck PJ, Behrendt N, Meijers JCM, von Drygalski A, Mosnier LO. Defective TAFI activation in hemophilia A mice is a major contributor to joint bleeding. Blood. 2018; 132: 1593–1603. [PubMed: 30026184]
11. Casanova-Acebes M, Pitaval C, Weiss LA, Nombela-Arrieta C, Chevre R, N AG, Kunisaki Y, Zhang D, van Rooijen N, Silberstein LE, Weber C, Nagasawa T, Frenette PS, Castrillo A, Hidalgo A. Rhythmic modulation of the hematopoietic niche through neutrophil clearance. Cell. 2013; 153: 1025–1035. [PubMed: 23706740]
12. Notta F, Doulatov S, Laurenti E, Poeppl A, Jurisica I, Dick JE. Isolation of single human hematopoietic stem cells capable of long-term multilineage engraftment. Science. 2011; 333: 218–221. [PubMed: 21737740]

13. Macosko EZ, Basu A, Satija R, Nemesh J, Shekhar K, Goldman M, Tirosh I, Bialas AR, Kamitaki N, Martersteck EM, Trombetta JJ, Weitz DA, Sanes JR, Shalek AK, Regev A, McCarroll SA. Highly Parallel Genome-wide Expression Profiling of Individual Cells Using Nanoliter Droplets. Cell. 2015; 161: 1202–1214. [PubMed: 26000488]

14. Tirosh I, Izar B, Prakadan SM, Wadsworth MH 2nd, Treacy D, Trombetta JJ, Rotem A, Rodman C, Lian C, Murphy G, Fallahi-Sichani M, Dutton-Regester K, Lin JR, Cohen O, Shah P, Lu D, Genshaft AS, Hughes TK, Ziegler CG, Kazer SW, Gaillard A, Kolb KE, Villani AC, Johannessen CM, Andreev AY, Van Allen EM, Bertagnolli M, Sorger PK, Sullivan RJ, Flaherty KT, Frederick DT, Jane-Valbuena J, Yoon CH, Rozenblatt-Rosen O, Shalek AK, Regev A, Garraway LA. Dissecting the multicellular ecosystem of metastatic melanoma by single-cell RNA-seq. Science. 2016; 352: 189–196. [PubMed: 27124452]

15. Butler A, Hoffman P, Smibert P, Papalexi E, Satija R. Integrating single-cell transcriptomic data across different conditions, technologies, and species. Nat Biotechnol. 2018; 36: 411–420. [PubMed: 29608179]

16. L W, N vE A smart local moving algorithm for large-scale modularity-based community detection. The European Physical Journal B. 2013; 86: 471.

17. Becht E, McInnes L, Healy J, Dutertre CA, Kwok IWH, Ng LG, Ginhoux F, Newell EW. Dimensionality reduction for visualizing single-cell data using UMAP. Nat Biotechnol. 2018.

18. Geiger H, Pawar SA, Kerschen EJ, Nattamai KJ, Hernandez I, Liang HP, Fernandez JA, Cancelas JA, Ryan MA, Kustikova O, Schambach A, Fu Q, Wang J, Fink LM, Petersen KU, Zhou D, Griffin JH, Baum C, Weiler H, Hauer-Jensen M. Pharmacological targeting of the thrombomodulin-activated protein C pathway mitigates radiation toxicity. Nat Med. 2012; 18: 1123–1129. [PubMed: 22729286]

19. Gekas C, Graf T. CD41 expression marks myeloid-biased adult hematopoietic stem cells and increases with age. Blood. 2013; 121: 4463–4472. [PubMed: 23564910]

20. Isermann B, Vinnikov IA, Madhusudhan T, Herzog S, Kashif M, Blautzik J, Corat MA, Zeier M, Blessing E, Oh J, Gerlitz B, Berg DT, Grinnell BW, Chavakis T, Esmon CT, Weiler H, Bierhaus A, Nawroth PP. Activated protein C protects against diabetic nephropathy by inhibiting endothelial and podocyte apoptosis. Nat Med. 2007; 13: 1349–1358. [PubMed: 17982464]

21. Peters M, Schirmacher P, Goldschmitt J, Odenthal M, Peschel C, Fattori E, Ciliberto G, Dienes HP, Meyer zum Buschenfelde KH, Rose-John S. Extramedullary expansion of hematopoietic progenitor cells in interleukin (IL)-6-sIL-6R double transgenic mice. J Exp Med. 1997; 185: 755–766. [PubMed: 9034153]

22. Suematsu S, Matsuda T, Aozasa K, Akira S, Nakano N, Ohno S, Miyazaki J, Yamamura K, Hirano T, Kishimoto T. IgG1 plasmacytosis in interleukin 6 transgenic mice. Proc Natl Acad Sci U S A. 1989; 86: 7547–7551. [PubMed: 2798426]

23. Peters M, Solem F, Goldschmidt J, Schirmacher P, Rose-John S. Interleukin-6 and the soluble interleukin-6 receptor induce stem cell factor and Flt-3L expression in vivo and in vitro. Exp Hematol. 2001; 29: 146–155. [PubMed: 11166453]

24. Wilson NK, Kent DG, Buettner F, Shehata M, Macaulay IC, Calero-Nieto FJ, Sanchez Castillo M, Oedekoven CA, Diamanti E, Schulte R, Ponting CP, Voet T, Caldas C, Stingl J, Green AR, Theis FJ, Gottgens B. Combined Single-Cell Functional and Gene Expression Analysis Resolves Heterogeneity within Stem Cell Populations. Cell Stem Cell. 2015; 16: 712–724. [PubMed: 26004780]

25. Baumer N, Krause A, Kohler G, Lettermann S, Evers G, Hascher A, Baumer S, Berdel WE, Muller-Tidow C, Tickenbrock L. Proteinase-Activated Receptor 1 (PAR1) regulates leukemic stem cell functions. PLoS One. 2014; 9: e94993. [PubMed: 24740120]

26. Lopez ML, Soriano-Sarabia N, Bruges G, Marquez ME, Preissner KT, Schmitz ML, Hackstein H. Expression pattern of protease activated receptors in lymphoid cells. Cell Immunol. 2014; 288: 47–52. [PubMed: 24637088]

27. Lenkiewicz A, Bujko K, Brzezniakiewicz-Janus K, Xu B, Ratajczak MZ. The Complement Cascade as a Mediator of Human Malignant Hematopoietic Cell Trafficking. Front Immunol. 2019; 10: 1292. [PubMed: 31231394]

28. Pepler L, Yu P, Dwivedi DJ, Trigatti BL, Liaw PC. Characterization of mice harboring a variant of EPCR with impaired ability to bind protein C: novel role of EPCR in hematopoiesis. Blood. 2015; 126: 673–682. [PubMed: 26045607]

29. Ghosh S, Pendurthi UR, Steinoe A, Esmon CT, Rao LV. Endothelial cell protein C receptor acts as a cellular receptor for factor VIIa on endothelium. J Biol Chem. 2007; 282: 11849–11857. [PubMed: 17327234]

ESSENTIALS

- Differential activation of protease activated receptor 1 by activated protein C or thrombin has been reported to regulate hematopoietic stem cell function under homeostatic, steady-state conditions
- Thrombomodulin expression endows murine hematopoietic stem and progenitor cells with the capacity for quasi-autocrine maintenance of quiescence and bone marrow retention via aPC-biased activation of protease activated receptor 1
- The function of Thrombomodulin in murine hematopoietic stem cells was investigated in animal models with constitutive and temporally controlled Thrombomodulin deficiency
- Hematopoietic cell Thrombomodulin had only minor effects on constitutive hematopoiesis and stem cell function in the absence of hematopoietic stress signals in mice, and was not expressed in human stem cells

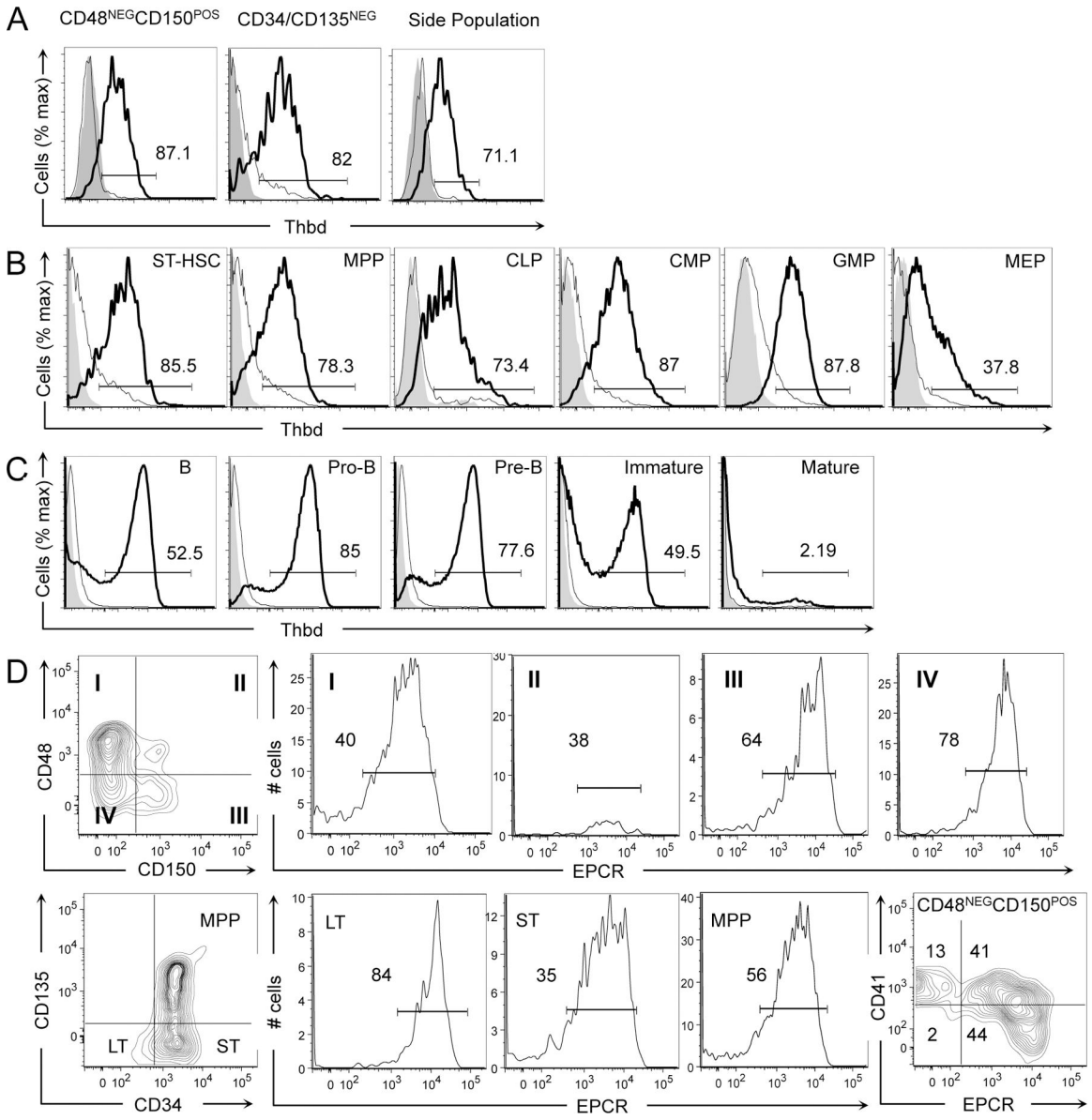

Figure 1: Thbd is expressed by all HSPC populations and immature B cells in the mouse BM.

(**A**) Histograms show Thbd expression on LT-HSC (LSK-CD34^{-}CD135^{-}), SLAM-HSC (LSK-CD48^{-}CD150^{+}), or the EPCR^{POS} side population (LSK-SP) Data shown are representative of 4 animals. (**B**) Thbd expression on ST-HSC (LSK-CD34^{+}CD135^{-}), MPP (LSK-CD34^{+}CD135^{+}), CLP (Lin^{-}Sca-1^{lo}c-Kit^{lo}IL7Ra^{+}), CMP (Lin^{-}Sca-1^{-}c-Kit^{+}CD34^{+}CD16/32^{-}), GMP (Lin^{-}Sca-1^{-}c-Kit^{+}CD34^{+}CD16/32^{+}), and MEP (Lin^{-}Sca-1^{-}c-Kit^{+}CD34^{-}CD16/32^{-}). Data shown are representative of 4 animals. (**C**) Thbd expression on total B cells (B220^{+}CD19^{+}), Pro B cells (CD19^{+}B220^{lo}IgM^{-}CD43^{+}), Pre B cells (CD19^{+}B220^{lo}IgM^{-}CD43^{-}), immature B cells (CD19^{+}B220^{lo}IgM^{+}) and mature B cells (CD19^{+}B220^{hi}IgM^{+}). Shaded histograms in A-C represent isotype control, thick line wild type mice and thin line Thbd-deficient mice. Numbers represent percentages of cells in the corresponding gates. Data shown are representative of 4 animals per group. Data shown are representative of 4 animals. **(D)** EPCR expression on LSK cells gated for expression of

CD48/CD150 or CD34/CD135. Histograms show EPCR expression in the respective gates of the contour plots on the left. Data shown are representative of 4 animals. Plot in the lower right panel shows expression of EPCR and CD41 (Itgab2) in LSK-CD48^{NEG}CD150^{POS} SLAM-HSC of a 9 months old animal.

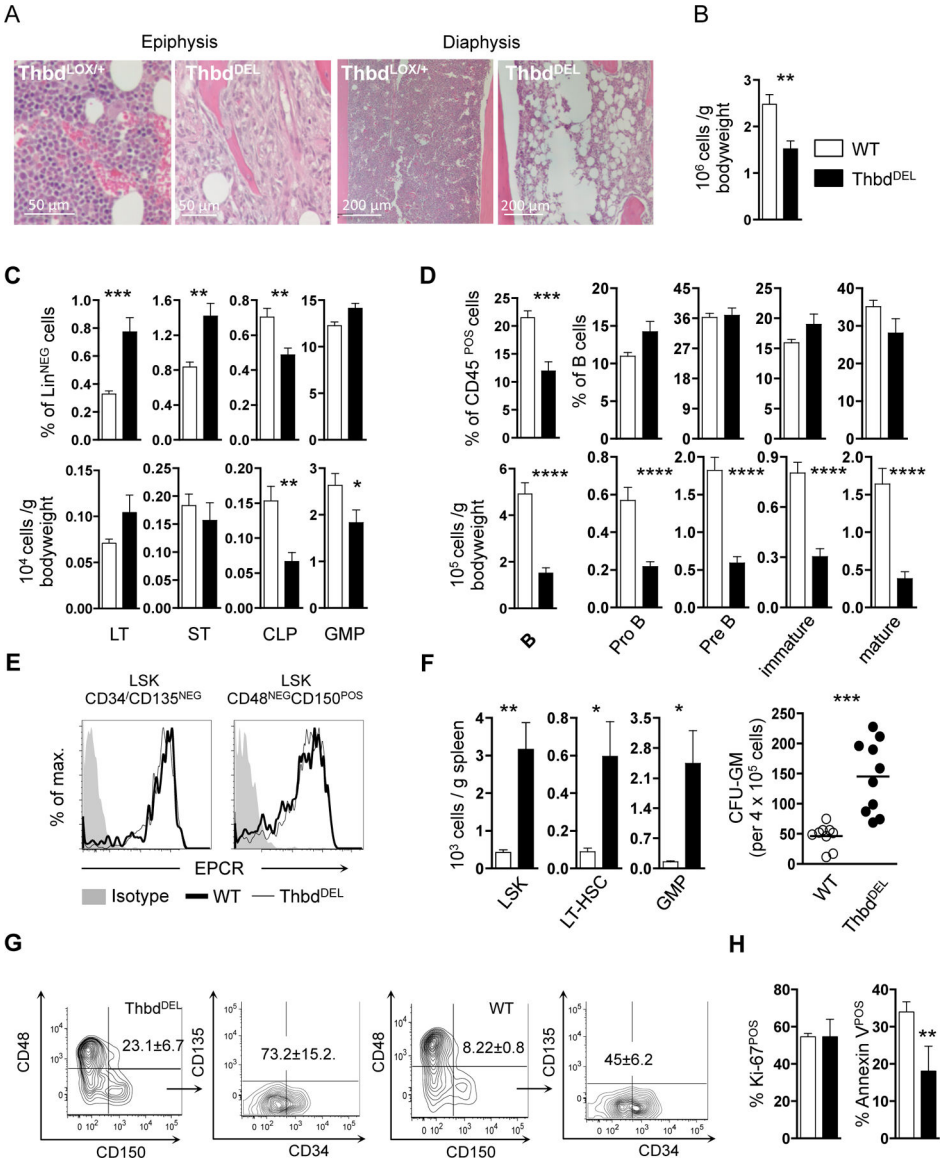

Figure 2: Characterization of HSPC in the bone marrow and spleen of Thbd-deficient mice.

(A) Bone marrow histology of Thbd^{DEL} mice. Formalin-fixed sections of femurs of Thbd, hematoxylin-eosin stain. **(B)** Reduced BM cellularity in Thbd^{DEL} mice (n=8/group). **(C,D)**. Frequency and absolute numbers of HSPC (**C**) and bone marrow B cells (D) in control (open bars; n=9) and Thbd^{DEL} mice (closed bars; n=8). LT: LSK-CD34^{-}CD135^{+}; ST: LSK-CD34^{+}CD135^{-}; MPP: LSK-CD34^{+}CD135^{+}; CLP: Lin^{-}Sca-1^{lo}c-Kit^{lo}IL7Rα^{+}; CMP: Lin^{-}Sca-1^{-}c-Kit^{+}CD34^{+}CD16/32^{-}; GMP: Lin^{-}Sca-1^{-}c-Kit^{+}CD34^{+}CD16/32^{+}; MEP, Lin^{-}Sca-1^{-}c-Kit^{+}CD34^{-}CD16/32^{-}. **(E)** Cytometry histograms showing normal EPCR expression in LT-HSC and SLAM-HSC of wildtype and Thbd^{DEL} mice. Data shown are representative of 4 animals/group. **(F)** Increased abundance of HSPC (left) and hematopoietic activity (Colony-forming-units Granulocyte-Monocyte) in the spleen of wildtype (open bars) and Thbd^{DEL} mice (closed bars; n=10/group). **(G)** Cytometry plots of CD48/CD150 expression on LSK cells of wildtype and Thbd^{DEL} mice. CD48^{NEG}CD150^{POS}

SLAM-HSC were then analyzed for CD34/CD135 expression (n=5/group). **(H)** Flow cytometric analysis of CD34/CD135^{NEG} LT-HSC for expression of the proliferation marker Ki67 and binding of annexin V to cell surface-associated phosphatidylserine as a marker of apoptosis (n=5/group). All numerical data are represented as mean±st.dev. Two-tailed, unpaired Student's t-test was performed to determine significance. *P < 0.05; **P < 0.01; ***P < 0.001; ****P < 0.0001.

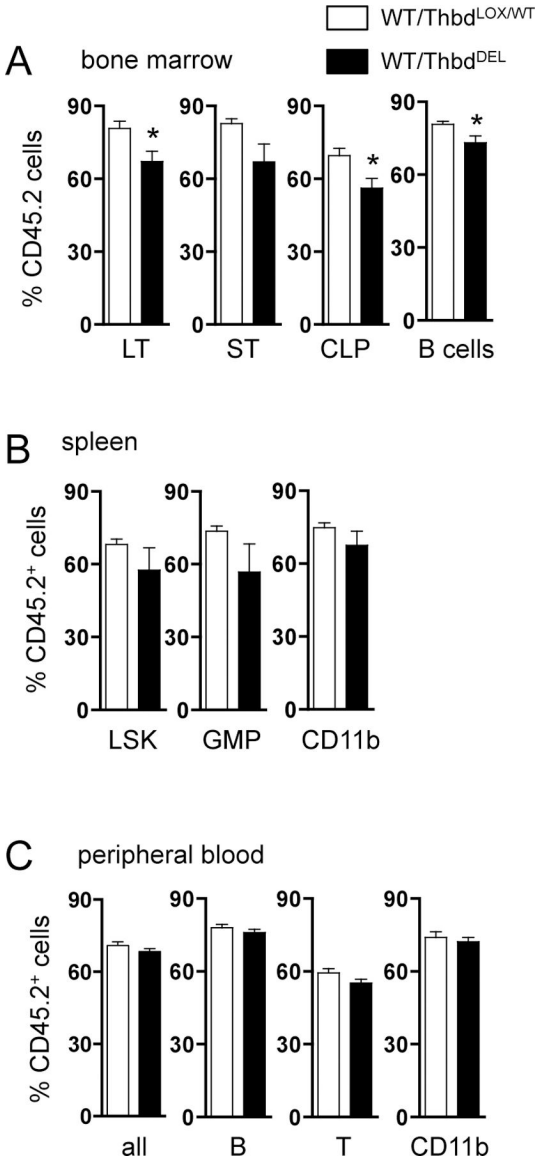

Figure 3: Thbd^{DEL} HSPC show near-normal competitive repopulation capacity.

Mixed BM chimera mice (n=6/group) were generated by transplanting BM from wild type (CD45.1) and either Thbd^{DEL}, or Thbd-expressing Thbd$^{LOX/WT}$ littermates (CD45.2) in a 1:1 ratio into lethally Boy/J recipients. CD45 chimerism was measured in the indicated tissues by flow cytometry 20 weeks after transplantation in (**A**) bone marrow (n=6/group), (**B**) spleen (n=6/group), and (**C**) peripheral blood (n=5/group). HSPCs in the BM and spleen were characterized as in Figure 1. Data represent the mean±SEM. Two-tailed unpaired t-test was used to determine significance. *P < 0.05.

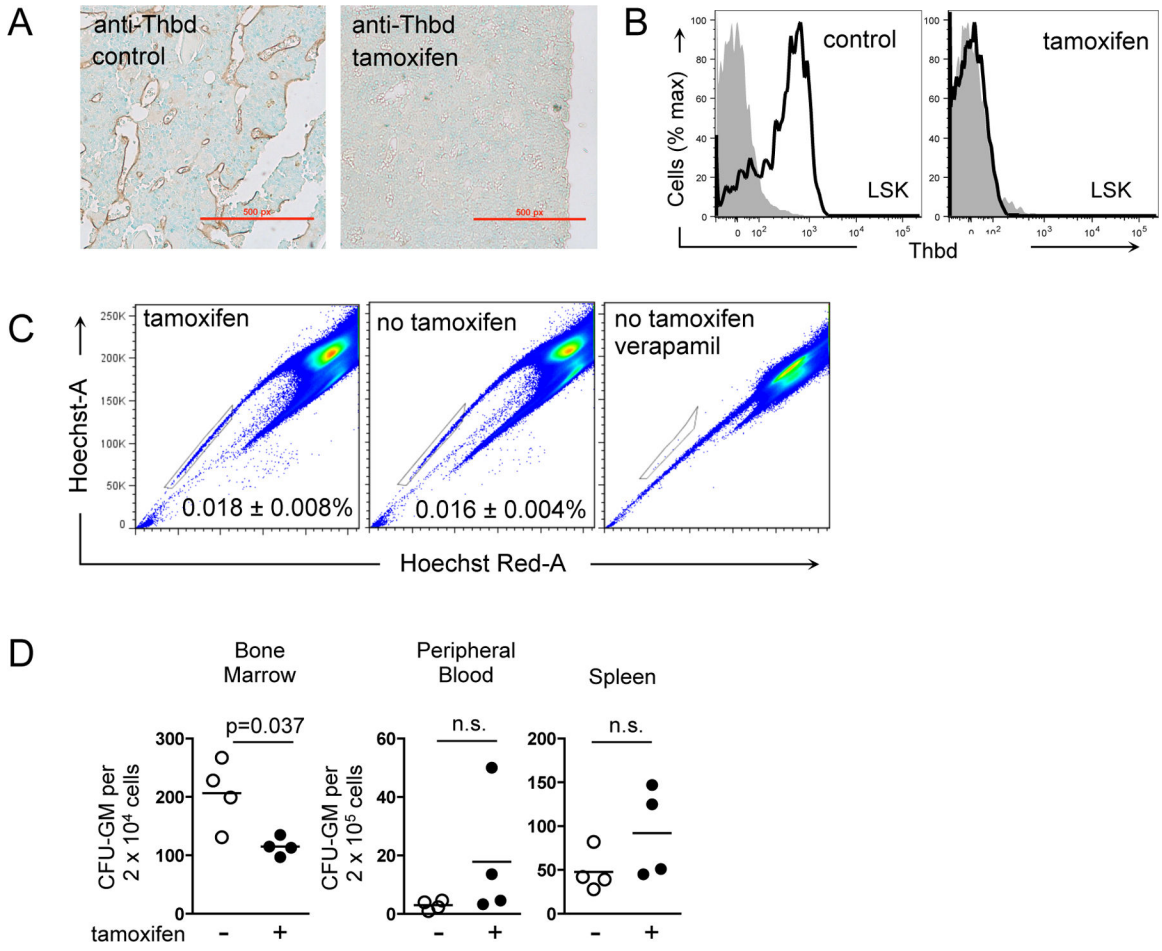

Figure 4: Temporally controlled Thbd gene ablation in adult mice.

(**A**) Immunohistochemical detection of Thbd antigen in BM blood vessels of formalin-fixed femur with HRP-conjugated anti-Thbd antibody. Counterstain hematoxylin. (**B**) Detection of Thbd antigen on $Lin^{NEG}Sca/kit^{POS}$ BM cells by flow cytometry. Tamoxifen-treatment abrogates Thbd expression on bone marrow HSPC. Data shown are representative of 4 animals/group analyzed (**C**) Tamoxin-induced Thbd gene ablation does not alter the abundance of side population HSC. Verapamil abolishes the Hoechst side population. Numbers are the mean±st.dev. of % side population cells. n=4/group. (**D**) Hematopoietic activity in the bone marrow, peripheral blood and spleen measured by colony formation in methylcellulose. Thbd gene ablation in adult mice is not associated with increased extramedullary hematopoiesis. Each data point reflects 1 animal.

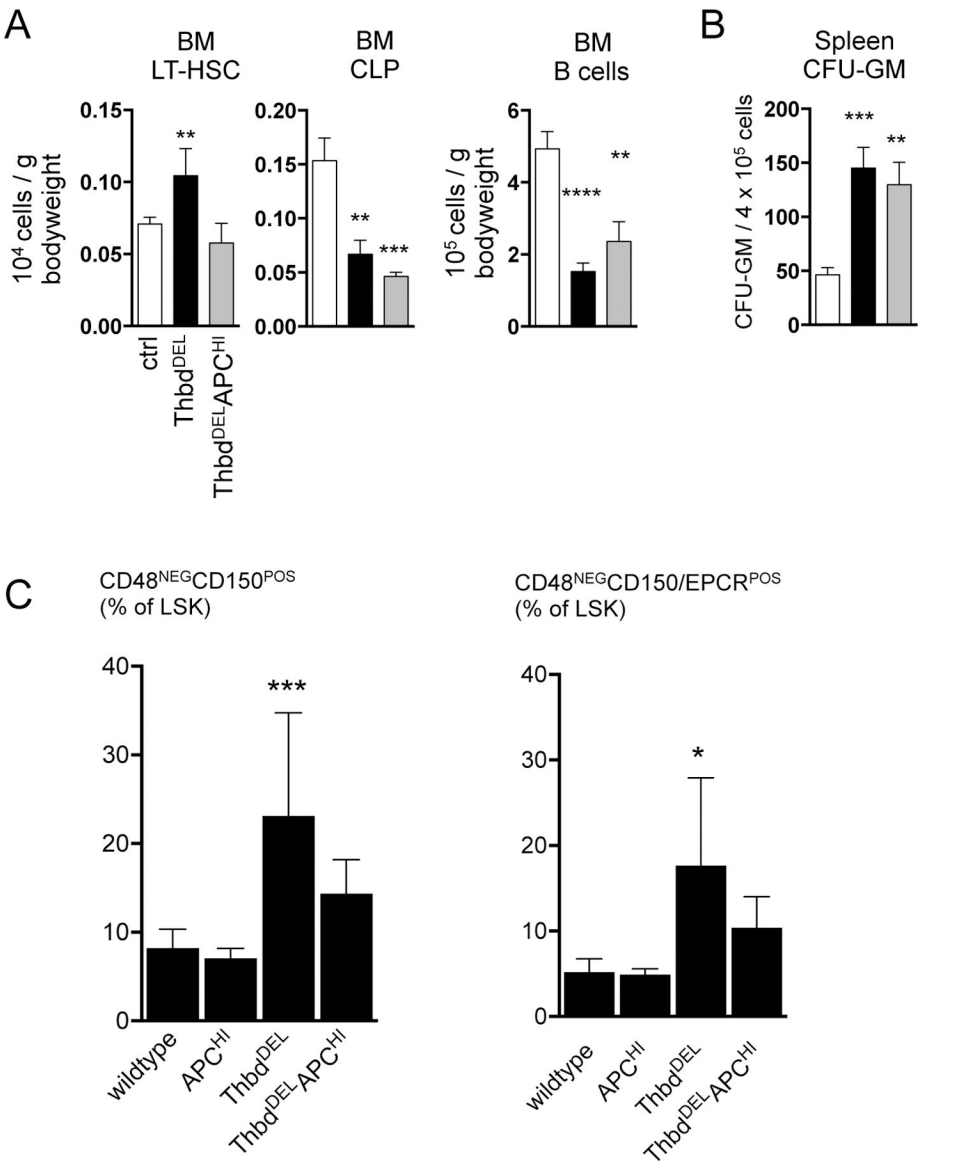

Figure 5: Transgenic aPC supplementation selectively restores normal HSC abundance.

(**A**) Flow cytometric evaluation of progenitor populations in the bone marrow of $Thbd^{DEL}$ mice (n=8), $Thbd^{DEL}APC^{HI}$ mice (n=7), and Thbd-expressing littermates ($Thbd^{LOX/WT}$; n=6). (**B**) Spleen hematopoietic activity determined by colony formation in methylcellulose. (**C**) Frequency (%) of SLAM-HSC and $EPCR^{POS}$ SLAM-HSC in wildtype (C57Bl/6N; n=9) mice and mutant strains (n=4/group). One-way ANOVA with Tukey's *post hoc* test was used to determine significance. *P < 0.05; **P < 0.01; ***P < 0.001; ****P < 0.0001.

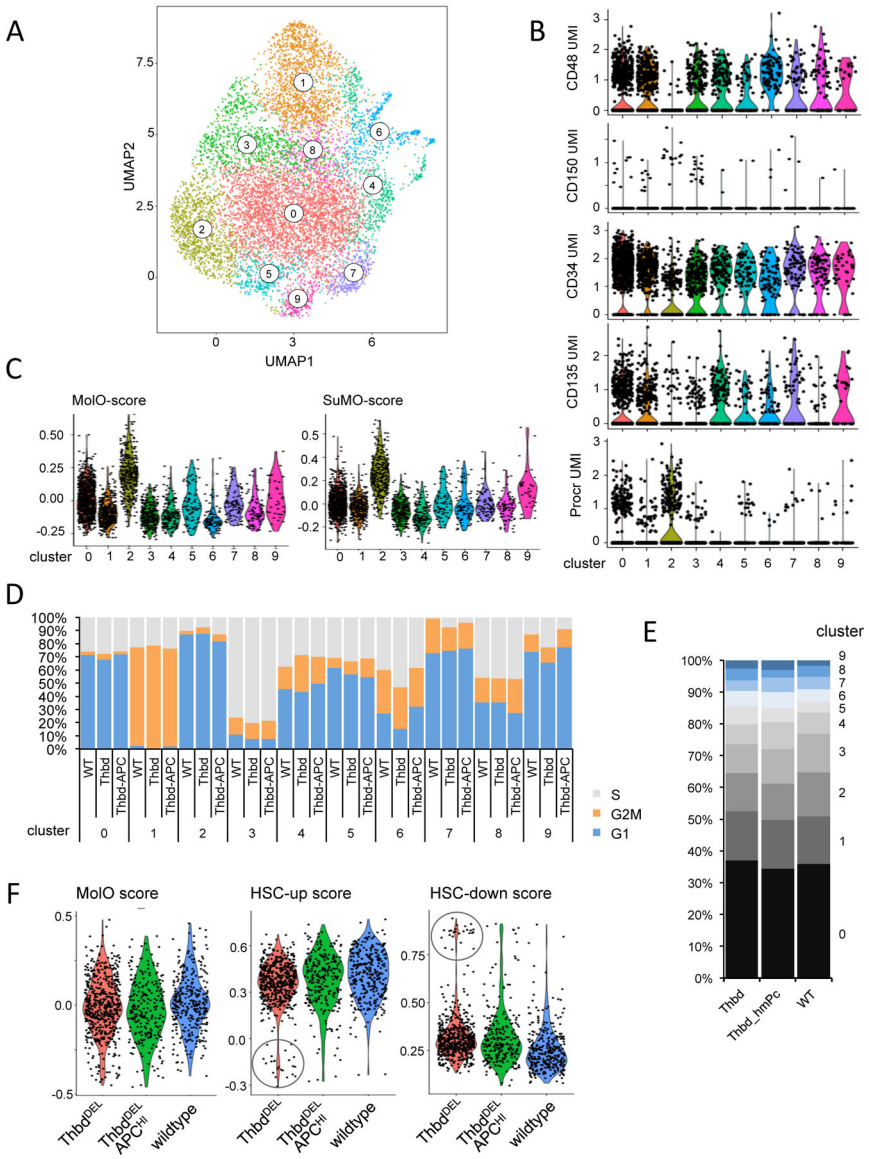

Figure 6: Single-cell RNA sequencing reveals largely similar LSK compartments across WT, Thbd^{DEL}, and Thbd^{DEL}APC^{HI} genotypes.

(A) UMAP overview of cell clustering across all cells from all genotypes. **(B)** Normalized expression values of LT-HSC markers across all clusters. **(C)** Collective expression of 'MolO' and 'SuMO' stem marker gene sets across all clusters. **(D)** Distribution of predicted cell cycle phases across all clusters and genotypes. **(E)** Percent contribution of cells from each genotype to each cluster. **(F)** Collective expression of HSC-up and HSC-down stem cell marker gene set within LT-HSC cells (cluster 2) across all genotypes. Circled cluster 2 cells show a marked loss of transcriptionally defined stemness and are predicated to be within S or G2M cell cycle phases.

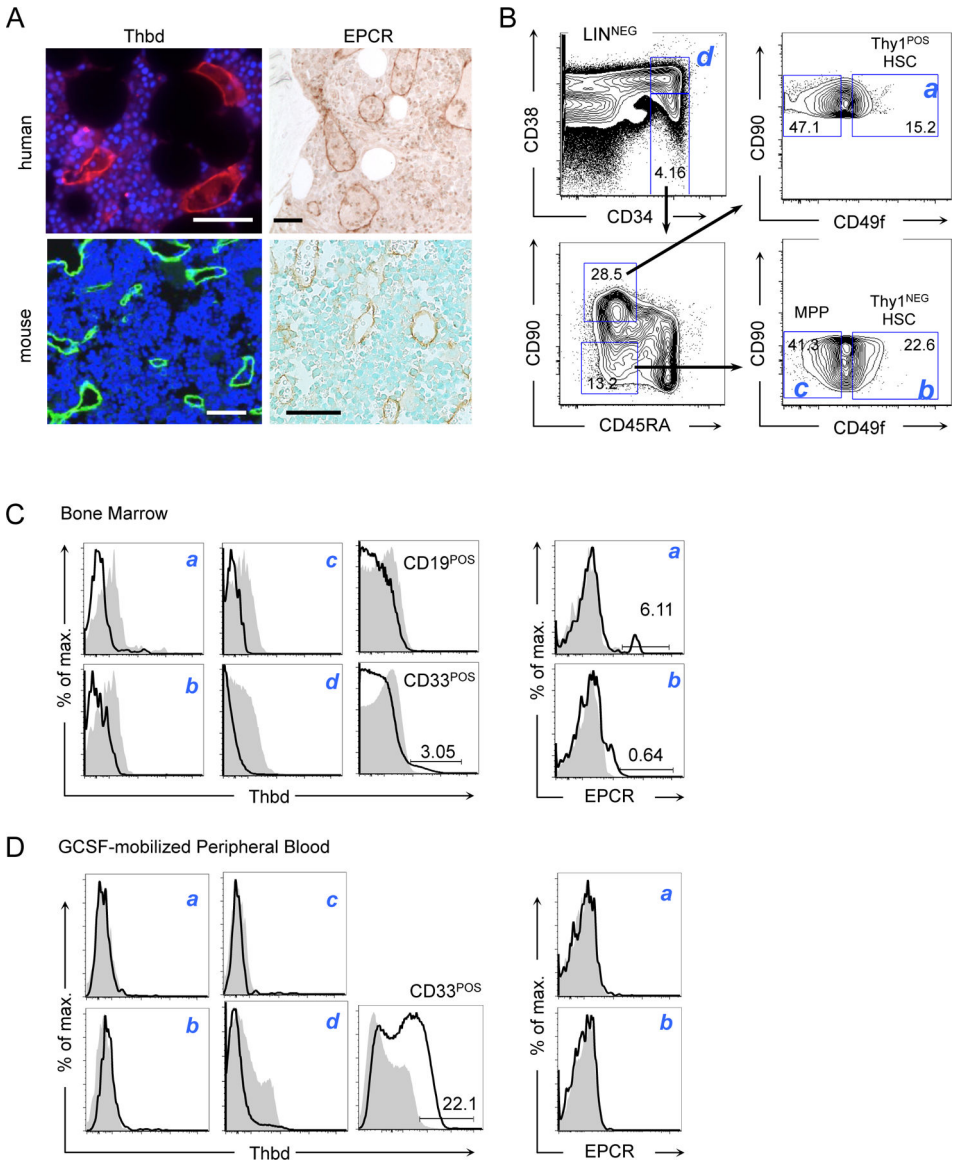

Figure 7. Thbd expression in human BM is restricted to the endothelial niche and a small fraction of myeloid cells.

(**A**) Immunohistochemical detection of Thbd (red/green fluorescence; nuclear counterstain with DAPI (blue)) and EPCR (brown HRP reaction product; Giemsa counterstain for human Thbd, no counterstain for human EPCR) in endothelial cells of human and mouse BM sections. Bars represent 50 μm. (**B**) Gating strategy for characterization of Thbd and EPCR expression in HSPC by flow cytometry in human BM and peripheral blood[12]: Gate "**a**" and "**b**": HSC enriched (CD38/CD45RA^{NEG}CD90/CD34/CD49f^{POS} and CD38/CD45RA/CD90^{NEG}CD34/CD49f^{POS}). Gate "**c**": MPP (CD38/CD45RA/CD90^{NEG}CD34/CD49f^{NEG}). Gate "**d**": Lineage-restricted progenitors (CD34/CD38^{POS}). (**C, D**) Flow cytometric detection of Thbd and EPCR in BM (C) and peripheral blood of GCSF-mobilized donors (D). Histograms show expression in the indicted gating populations a–d, or in B and myeloid cells (CD19^{POS} and CD33^{POS}, respectively). Numbers represent percentage of cells in the corresponding gates. Data are one representative of two human BM samples, and two

peripheral blood samples analyzed. Shaded histogram areas represent isotype controls, black line represents anti-Thbd or -EPCR antibody.